



## Influence of varying timing angle on performance of an SI engine: An experimental and numerical study

A. H. Kakaee<sup>a,\*</sup> and J. Zareei<sup>b</sup>

<sup>a</sup>Department of Automotive Engineering, Iran University of Science and Technology, Iran

<sup>b</sup>Engineering Center for Technical Drawing, Sharif University of Technology, Iran

### Article info:

Received: 29/09/2012

Accepted: 15/01/2013

Online: 03/03/2013

### Keywords:

Engine ignition timing,  
Two zones,  
Burned and unburned  
gasses,  
Emissions.

### Abstract

Engine performance depends on two main factors of engine speed and ignition time. Ignition timing can affect engine life, fuel economy and engine power. In this paper, to study engine performance of Peugeot 206 TU3A with comparison ratio of 10.5:1 and displacement of 1361CC in MATLAB software, a two-zone burned/unburned model with the fuel burning rate described by aWiebe function was used for modeling in-cylinder combustion. For studying this issue, thermodynamic models such as Woshni, Isentropic, etc. were used. Then, the experiments were carried out to validate the calculated data. The objective of the present work was to examine effect of ignition timing on the performance of an SI engine. For achieving this goal, at the speed of 3400 rpm, ignition timing was changed in the range of 41 degrees before the top dead centre to 10 degrees after TDC. By changing the ignition timing, the results of some characteristics such as power, torque, indicatory pressure, exhaust emission and efficiency were obtained and compared. The results demonstrated that optimal power and torque and the maximum efficiency were achieved at 31 degrees before the top dead centre and engine performance was improved by changing timing angle. It was also indicated that the maximum thermal efficiency could be accomplished while peak pressure occurred between 5 and 15 degrees of ATDC. The amounts of O<sub>2</sub>, CO<sub>2</sub> and CO were almost constant but HC increased with increase of ignition timing.

## 1. Introduction

Performance of spark ignition engines is a function of many factors, one of the most important of which is ignition timing. Furthermore, it is one of the most important parameters for optimizing efficiency and emissions, permitting combustion engines to conform to future emission targets and standards [1]. Since the advent of Otto's first

four stroke engine, development of the spark ignition engine has achieved a high level of success. In the early years, increasing engine power and engine working reliability were the principal aims for engine designers. In recent years, however, ignition timing has brought increased attention to development of advanced SI engines for maximizing performance [2]. Chan and Zhu worked on modeling in-cylinder thermodynamics under high values of ignition

---

\*Corresponding author

Email address: [kakaee\\_ah@iust.ac.ir](mailto:kakaee_ah@iust.ac.ir)

retard, in particular effect of spark retard on cylinder pressure distribution. In cylinder gas temperature and trapped mass under varying spark timing conditions were also calculated. Soyulu and Gerpen developed a two zone thermodynamic model to investigate effects of ignition timing, fuel composition and equivalence ratio on burning rate and cylinder pressure for a natural gas engine. Burning rate analysis was carried out to determine flame initiation period and flame propagation period at different engine operating conditions [3].

Others used multi-dimensional reactive flow codes for elaborating modeling of engine flow and combustion processes, which were very sophisticated [4-5]. Accurate prediction of performance parameters and exhaust emissions depends on flow dynamics in the intake manifold, heat transfer and ignition timing. It is feasible to model all these processes with multi-dimensional flow codes coupled with detailed chemical kinetic mechanisms using experimental data. The KIVA-CHEMKIN combination is an example for the detailed modeling of flow and combustion processes in internal combustion engines. However, multi-dimensional modeling of all these processes from the intake manifold to the exhaust manifold needs extensive computation time and very powerful computers. If these multi-dimensional reactive flow codes require large amounts of time, engine designers may not use them. Further, these codes are not still perfect and need some tuning with experimental data, which requires expertise and even more computer time. For this reason, the need for accurate predictions of exhaust emissions pollutants forced the researchers to attempt developing two zone combustion models [6-7]. Eventually, some multi-zone combustion models have appeared, carrying the expected drawbacks of the first attempts, where the detailed analysis of fuel-air distribution permits calculation of the exhaust gas composition with reasonable accuracy [8]. However, this happens under the rising computing time cost when compared to lower zones gasoline combustion models.

Therefore, it is a reasonable choice sounds to be a two zone combustion model, which includes

the effects of changes in engine design and operation on the details of the combustion process through a phenomenological model where the geometric details are fairly well approximated by detailed modeling of the different mechanisms involved. This is going to have the advantages of relative simplicity and very reasonable computer time cost.

Abdallah and Soliman worked on effect of injection timing on performance of a dual fuel engine and the results showed that low efficiency and poor emission at light loads can be improved significantly by advancing injection timing of the pilot fuel [9]. Also, experimental research on performance of hydrogen fueled engine was carried out under the condition of different ignition timing and injection timing [10]. Thus, performances and emissions in the spark ignition engine attain optimization in every operating state of the engine.

The objective of the present work was to examine effect of ignition timing on performance of an SI engine. To achieve this goal, testing was conducted at 3400 rpm and wide open throttle, ignition timing was changed in the range of 10° ATDC to 41° BTDC and performance characteristics such as power, torque, thermal efficiency, pressure and heat release were obtained and compared.

## 2. Test engine

Facilities for monitoring and controlling engine variables such as engine speed, engine load, water and lube oil temperatures, fuel and air flows etc, were installed on a fully automated test bed, four cylinder, water cooled, naturally aspirated SI engine with experimental standard which was located at laboratory of Iran Khodro Company. Specifications of the test engine are given in Table 1.

The engine was mounted on a fully automated test bed and coupled with a Schenck W130 eddy current dynamometer with load absorbing and motoring capabilities. There was one electric sensor for speed and one for load, with these signals fed for indicators on the control panel and to the controller. Via the knobs on the control panel, the operator could set the

dynamometer to control speed or load. There was also the capability of setting ignition timing from a switch on the control panel. Also, for manually changing timing angle with interval of 10 degrees, the valves were opened and reset.

**Table 1.** Engine specifications.

Engine type	TU3A
Number of strokes	4
Number of cylinders	4
Cylinder diameter (mm)	75
Stroke (mm)	77
Compression ratio	10.5:1
Maximum power (kW)	50
Maximum Torque (NM)	160
Maximum speed (rpm)	6500
Displacement (cc)	1360
Fuel	97-octane

The coolant and lube oil circulation were achieved by electrically driven pumps at the temperature controlled by water fed heat exchangers. Heaters were used to maintain the oil and coolant temperatures during the warm up and light load conditions. Figure 1 shows the tested engine.

### 3. Model description

A zero-dimensional thermodynamic cycle model with two-zone burned/unburned combustion model, mainly based on Ferguson's work, was developed to predict the cylinder pressure, work done, heat release, enthalpy of exhaust gas, etc. The zero-dimensional model was based on the first law of thermodynamics in which an empirical relationship between fuel burning rate and crank angle position was established. Figure 2 shows the burned and unburned zones, which were presumed to be separated by an infinitesimally thin flame front. The burned zone consisted of the equilibrium products of combustion and both zones were assumed to be at the same pressure at any CA degree. The region in the combustion chamber was treated as a control volume. The governing equations included mass and energy conservation equations and equations of state. These equations, with crank angle as the independent variable, formed building block of this thermodynamic model.



**Fig. 1.** The tested engine.

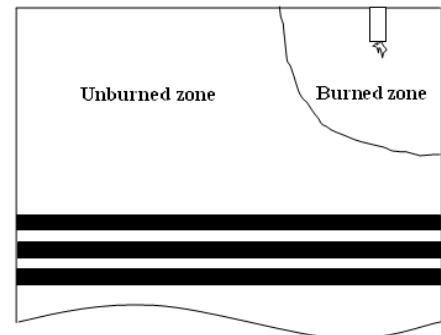


**Fig. 2.** Burned and unburned zones of combustion chamber.

### 4. Numerical analysis

In order to determine transient heat flux,  $Q$ , in combustion chamber during combustion process, heat transfer was considered a function of crank angle,  $\theta$ , as follows:

$$\frac{dQ}{d\theta} = \frac{-Q_1}{\omega} = \frac{-Q_b - Q_u}{\omega} \quad (1)$$

The combustion chamber exhaust gasses of internal combustion engines were divided into two zones of burned and unburned gasses. where  $Q_b$  and  $Q_u$  are heat transfer ratio for burned and unburned gasses, respectively, and  $Q_1$  is sum of  $Q_b$  and  $Q_u$ . Burned and unburned gasses are functions of temperature defined as shown below (2):

$$Q_b = hA_b(T_b - T_w) \quad (2)$$

$$Q_u = hA_u(T_u - T_w) \quad (3)$$

where  $h$  is a coefficient of convection heat transfer in standard,  $T_w$  is contact temperature,  $A_b$  and  $A_u$  are burned gasses to the wall cylinder's contact surface and unburned gasses to the wall cylinder's contact surface, respectively, as follows (1):

$$A_b = \left(\frac{\pi b^2}{2} + \frac{4V}{b}\right)x^{\frac{1}{2}} \quad (4)$$

$$A_u = \left(\frac{\pi b^2}{2} + \frac{4V}{b}\right)^{1-x^{\frac{1}{2}}} \quad (5)$$

The wall cylinder's temperature reached 450 degrees of Kelvin. This temperature was the maximum working temperature of the lubricant oil (5).

Equations (4) and (5) were practical functions.  $x$  is a burned gasses partial mass in cylinder and  $V$  is combustion chamber's volume. Equation (4) and (5) were empirical functions that had the correct limits in the case of a cylinder where  $x \rightarrow 0$  and when  $x \rightarrow 1$ . Burned gasses always occupy a large part of the cylinder's volume.

$h_c$  is correction coefficient of  $h$  (during the engine operation) introduced by Woschni as follows (5):

$$h_c = 3.26 B^{-0.2} P^{0.8} w^{0.8} T^{-0.55} \quad (6)$$

where  $B$  is cylinder bore,  $T$  is temperature,  $P$  is pressure and  $w$  is mean velocity for the gas in the cylinder. The mean velocity of gas was in proportion to the mean piston velocity during the intake, compression and exhaust strokes. The average cylinder gas velocity,  $w$ , for a 4-stroke engine without swirl determined by Woschni was (4):

$$w = C_1 S_p + C_2 \left[ \frac{V_d T_r}{P_r V_r} \right] (P - P_m) \quad (7)$$

$C_1 = 2.28$ ,  $C_2 = 0$ , 0 during the compression stroke

$C_1 = 2.28$ ,  $C_2 = 0.00324$  during the combustion and expansion stroke

$P_r$ ,  $V_r$  and  $T_r$  are initial states for cylinder.  $V_d$  is piston displacement and  $S_p$  is mean velocity of piston. To determine mean gas velocity, the pressure and temperature values in all cycles were needed. Each of the above parameters was a function of thermodynamic properties based upon the first law of thermodynamics (2).

$$\Delta U = Q - W \quad (8)$$

Herein, variation of each system internal energy was equal to the difference between heat transfer and work generated by the system. Differential equation forms of (8) became:

$$m \frac{du}{d\theta} + u \frac{dm}{d\theta} = \frac{dQ}{d\theta} - P \frac{dV}{d\theta} - \frac{m_1 h_1}{\omega} \quad (9)$$

where  $m_1$  is mass flow ratio,  $h_1$  is inlet enthalpy,  $u$  is internal energy and  $\omega$  is engine's rotational speed. In the above equation, cylinder volume is assumed as control volume.

#### 4.1. Specific internal energy

Thermodynamical properties of engine cycles, internal energy-enthalpy and specific heat are functions of pressure and temperature. Furthermore, burned gasses are made of ten elements, obtainable from the balanced chemical equation for a combustion reaction. The equation of a specific internal energy of a system is:

$$v = \frac{U}{m} = xv_b + (1-n)v_u \quad (10)$$

$u_b$  is a burned gasses' internal energy at temperature  $T_b$  and  $u_u$  is an unburned gasses' internal energy at temperature  $T_u$ . Burned gasses' energy is a function of pressure and temperature.

$$u_b = u_b(T_b, P) \quad (11)$$

and differential form of the above equation is:

$$\frac{du_b}{d\theta} = \frac{\partial u_b}{\partial T_b} \frac{dT_b}{d\theta} + \frac{\partial u_b}{\partial P} \frac{dP}{d\theta} \quad (12)$$

Logarithmic form of specific internal energy is:

$$\begin{aligned} \frac{du_b}{d\theta} = & \left( C_{pb} - \frac{P v_b}{T_b} \frac{\partial \ln v_b}{\partial \ln T_b} \right) \frac{dT_b}{d\theta} \\ & - v_b \left( \frac{\partial \ln v_b}{\partial \ln T_b} + \frac{\partial \ln v_b}{\partial \ln P} \right) \frac{dP}{d\theta} \end{aligned} \quad (13)$$

And, equation of unburned gasses is:

$$\frac{du_u}{d\theta} = \left( C_{pb} - \frac{P v_b}{T_u} \frac{\partial \ln v_u}{\partial \ln T_u} \right) \frac{dT_u}{d\theta} - v_u \left( \frac{\partial \ln v_u}{\partial \ln T_u} + \frac{\partial \ln v_u}{\partial \ln P} \right) \frac{dP}{d\theta} \quad (14)$$

#### 4.2. Specific volume

Specific volume of a system is defined as demonstrated below (6):

$$v = \frac{U}{m} = x v_b + (1 - x) v_u \quad (15)$$

The burned gasses' specific volume is a function of pressure and temperature.

$$v_b = v_b(T_b, P) \quad (16)$$

And, differential form of the equation:

$$\frac{dv_b}{d\theta} = \frac{\partial v_b}{\partial T_b} \frac{dT_b}{d\theta} + \frac{\partial v_b}{\partial P} \frac{dP}{d\theta} \quad (17)$$

Logarithmic form of specific volume is:

$$\frac{dv_b}{d\theta} = \frac{v_b}{T_b} \frac{\partial \ln v_b}{\partial \ln T_b} \frac{dT_b}{d\theta} + \frac{v_b}{P} \frac{\partial \ln v_b}{\partial \ln P} \frac{dP}{d\theta} \quad (18)$$

And the equation for unburned gasses:

$$\frac{dv_u}{d\theta} = \frac{v_u}{T_u} \frac{\partial \ln v_u}{\partial \ln T_u} \frac{dT_u}{d\theta} + \frac{v_u}{P} \frac{\partial \ln v_u}{\partial \ln P} \frac{dP}{d\theta} \quad (19)$$

#### 4.3. Enthalpy

During the engine operation, some gasses leak out of the cylinder through the rings. This mass loss causes enthalpy and engine efficiency reduction. Gas leakage through the rings occurs in two stages of unburned gasses before combustion process and burned gasses after combustion process.

In order to compensate for the mass loss, a correction coefficient was used.

To calculate the enthalpy based on changes in partial mass, the following equation was applied:

$$h_1 = (1 - x^2) h_u + x^2 h_b \quad (20)$$

Another form of enthalpy for burned and unburned gasses were as follows:

$$h_u = h_u(T_u, P) \quad , \quad h_b = h_b(T_b, P) \quad (21)$$

#### 4.4. Mass loss through the rings

Variation of mass due to the crank angle is given in Eq. (9). According to the mass conservation equation and mass loss caused by gas leakage through the rings, the mass ratio due to crank angle could be:

$$\frac{dm}{d\theta} = \frac{-Cm}{\omega} \quad (22)$$

Where  $\omega$  is rotational speed of engine and the constant  $c$  is related to the engine ring's design. For example, if total mass loss equals 2.5%, then  $c$  will equal 0.8.

#### 4.5. Partial mass, mass and the volume of a system

The burned partial mass was investigated under three situations of compression, combustion and expansion (1).

Before combustion/compression:

$$x=0 \quad (23)$$

During the combustion:

$$x = \frac{1}{2} \left\{ 1 - \cos \left[ \pi \frac{\theta - \theta_s}{\theta_b} \right] \right\} \quad (24)$$

After combustion/expansion:

$$x=1 \quad (25)$$

In Eq. (24),  $\theta_s$  is spark timing and  $\theta_b$  is burning time. The mass quantity due to the crank angle equation could be given as follows:

$$m = m_1 \exp[-C(\theta - \theta_1)/\omega] \quad (26)$$

where  $m_1$  is mass in the commencement of

compression stroke, i.e. 180 degrees before TDC and  $\theta_1$  is equal to 180 degrees before TDC. The cylinder volume is(5):

$$\frac{V}{V_d} = \frac{1}{r-1} + \frac{1}{2} \left\{ \frac{\frac{1}{a} + 1 - \cos \theta}{-\left[\left(\frac{1}{a}\right)^2 - \sin^2 \theta\right]^{1/2}} \right\} \quad (27)$$

Where  $V_d$  is cylinder volume at TDC, r is compression ratio and a is piston's displacement to connecting rod's length.

#### 4.6. Solution method

In Eq. (9), only the term work must be solved. The work done by the piston is calculated by multiple pressures to volume change. The change in pressure and the burned and unburned gasses' temperature due to the crack angle are a function of the change in crank angle, pressure and burned and unburned gasses' temperature (4).

$$\frac{dP}{d\theta} = f_1(\theta, P, T_b, T_u) \quad (28)$$

$$\frac{dT_b}{d\theta} = f_2(\theta, P, T_b, T_u) \quad (29)$$

$$\frac{dT_u}{d\theta} = f_3(\theta, P, T_b, T_u) \quad (30)$$

So, the equations made systems of equations in six variables. This system was solved using Matlab Software. The solution was based on Ronge-Kutta method (4).

$$\frac{dP}{d\theta} = \frac{A + B + C}{D + E} \quad (31)$$

$$\frac{dT_b}{d\theta} = \frac{-h\left(\frac{\pi b^2}{2} + \frac{4V}{b}\right)x^{1/2}(T_u - T_u)}{\omega m c_{p_b^x}} + \frac{v_b}{C_{p_b}} \frac{\partial \ln v_b}{\partial \ln T_b} \left(\frac{A + B + C}{D + E}\right) + \frac{h_u - h_b}{XC_{p_b}} \left[\frac{dx}{d\theta} - (x - x^2)\frac{C}{\omega}\right] \quad (32)$$

$$\frac{dT_u}{d\theta} = \frac{-h\left(\frac{\pi b^2}{2} + \frac{4V}{b}\right)(1 - x^{1/2})(T_u - T_u)}{\omega m c_{p_u^{(1-x)}}} + \frac{v_u}{C_{p_u}} \frac{\partial \ln v_u}{\partial \ln T_u} \left(\frac{A + B + C}{D + E}\right) \quad (33)$$

$$\frac{dW}{d\theta} = P \frac{dV}{d\theta} \quad (34)$$

$$\frac{dQ_1}{d\theta} = \frac{h}{\omega} \left(\frac{\pi b^2}{2} + \frac{4V}{b}\right) \quad (35)$$

$$\left[x^{1/2}(T_b - T_u) + (1 - x^{1/2})(T_u - T_w)\right]$$

$$\frac{dH_1}{d\theta} = \frac{Cm}{\omega} [(1 - x^2)h_u + x^2h_b] \quad (36)$$

$$A = \frac{1}{m} \left(\frac{dV}{d\theta} + \frac{VC}{\omega}\right) \quad (37)$$

$$B = h \frac{\left(\frac{\pi b^2}{2} + \frac{4V}{b}\right)}{\omega m} \quad (38)$$

$$\left(\frac{v_b}{C_{p_b}} \frac{\partial \ln v_b}{\partial \ln T_b} x^{1/2} \frac{T_b - T_w}{T_b} + \frac{v_u}{C_{p_u}} \frac{\partial \ln v_u}{\partial \ln T_u} (1 - x^{1/2}) \frac{T_u - T_w}{T_u}\right)$$

$$C = (v_b - v_u) \frac{dx}{d\theta} v_b \frac{\partial \ln v_b}{\partial \ln T_b} \frac{h_u - h_b}{C_{p_b} T_b} \left[\frac{dx}{d\theta} \frac{(x - x^2)C}{\omega}\right] \quad (39)$$

$$D = x \left[\frac{v_b^2}{C_{p_b} T_b} \left(\frac{\partial \ln v_b}{\partial \ln T_b}\right)^2 + \frac{v_b}{P} \frac{\partial \ln v_b}{\partial \ln P}\right] \quad (40)$$

$$E = (1 - x) \left[\frac{v_u^2}{C_{p_u} T_u} \left(\frac{\partial \ln v_u}{\partial \ln T_u}\right)^2 + \frac{v_u}{P} \frac{\partial \ln v_u}{\partial \ln P}\right] \quad (41)$$

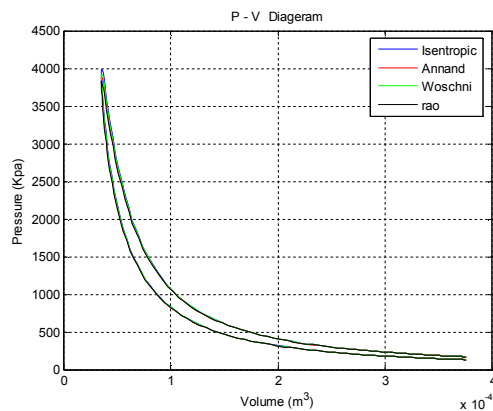
(32) and (33) were principal equations of this study. To calculate heat transfer coefficient based on Woschni method, pressure and temperature changes of burned gasses were

needed. Engine's geometrical parameters such as cylinder bore, piston displacement and compression ratio were used for engine's cycle simulation. Air-fuel ratio, ignition timing and initial pressure data were obtained from experimental conclusions and used for engine modeling.

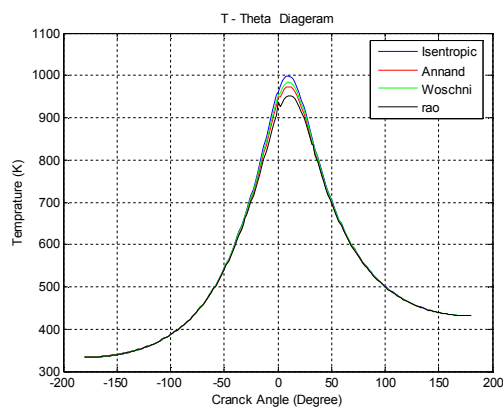
**5. Discussing modeling results**

Figure 3 shows a four-stroke cycle of TU3 engine with natural breathing in WOT condition and 31 degrees of timing. This cycle is similar in most passenger cars and other SI four-stroke engines.

The most important point in this engine is thermodynamic stability of various models. Consequently, the following diagram is fully compatible with Otto's diagram.



**Fig. 3.** Pressure–volume indicatory diagram in TU3 engine.



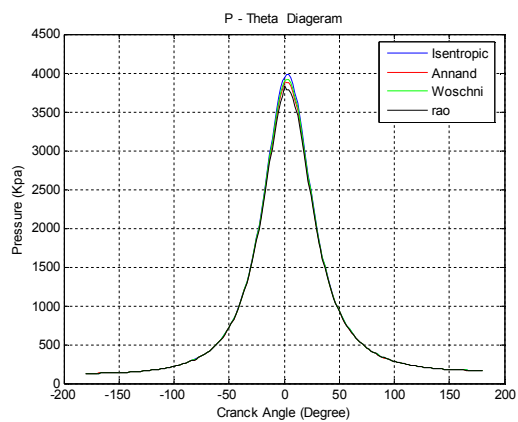
**Fig. 4.** Created temperature in combustion chamber versus crank angle.

Figure 4 shows the temperature generated within a combustion chamber versus crank angle using the discussed four models. As can be seen, the maximum temperature fell by about 5 degrees after TDC. Previous studies have shown that, if the maximum temperature fell by 3 to 10 degrees after TDC, the maximum possible efficiency can be achieved for any engine. Therefore, the above conditions showed that performance of this engine was fully positive and the maximum temperature was obtained by the isentropic model.

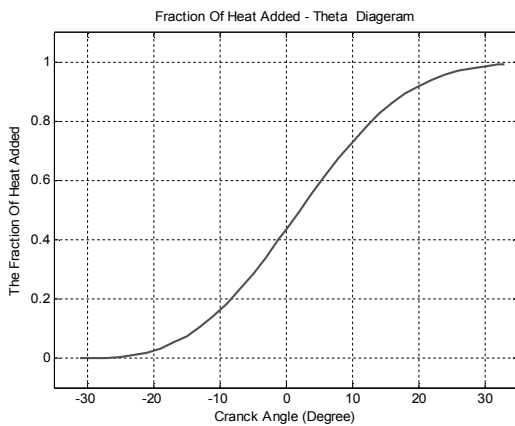
Figure 5 shows cylinder pressure variations in the combustion chamber as a function of crank angle. The increase of pressure after ignition and during flame spread was slow, which led to less increase of pressure force on engine piston and finally an engine with smooth operation and less noise.

The maximum pressure was obtained right after the top dead center; so engine efficiency was suitable and its combustion was complete. Consequently, pressure and temperature obtained in this engine created an ideal condition for decreasing exhaust emissions. In this diagram, the maximum pressure was related to isentropic diagram, i.e. close to Woschni model; as a result, each one of the used models is suitable for simulation of this engine.

Figure 6 shows fraction of heat added versus crank angle. Mechanical friction between dynamic parts was a main loss of generative power by the engine.



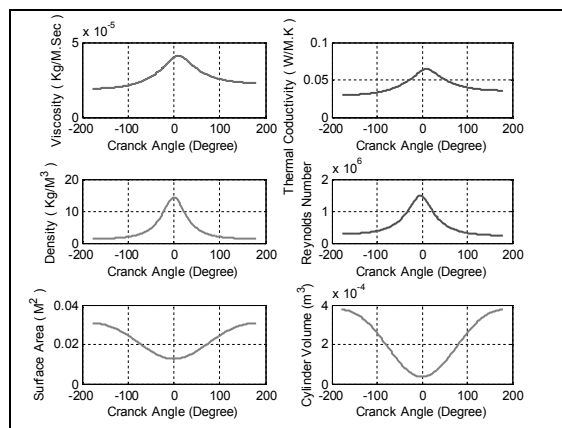
**Fig. 5.** Cylinder pressure variations in the combustion chamber as a function of crank angle.



**Fig. 6.** Variations increase heat due to friction versus crank angles.

A large percentage of mechanical friction was created by piston displacement within the cylinders. Other losses were related to friction as a result of fluid movement in the inlet and exhaust parts of gases, pass flow of valves and gas movement within the combustion chamber. Therefore, the engine needed a lubrication system for minimizing friction and engine abrasion. Two factors of piston movement towards the center and created heat increased result of friction, which affected loss of engine efficiency.

For solving this problem, the oil system can be used in different parts of the engine, right engine oil and improvement of cooling system.



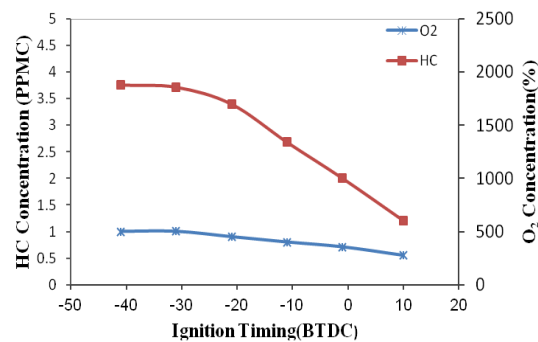
**Fig. 7.** Indicator diagram for a Peugeot 206 engine.

Figure 7 shows thermal conductivity, viscosity, density, Reynolds number, cylinder volume and contact surface of cylinder gases as a function of crank angle.

The above diagram shows that minimum and maximum values were obtained in top dead centers. Ultimately, the amounts of net work and effective efficiency in this engine were 602 Kj and 59.28 percent, respectively.

Table 2 shows operation of the TU3A engine in a condition that timing angle changed and also the things happened for the engine in the combustion chamber. In the above table, ignition time could vary from 41 to 11 degrees before the top dead center. Furthermore, it can be seen that 31 degree condition was suitable and ideal for this engine.

### 6. Discussing experimental results



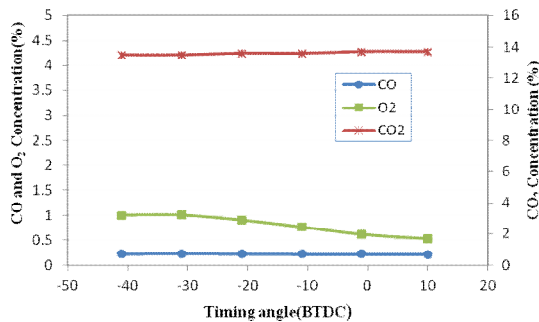
**Fig. 8.** Relationship between O<sub>2</sub> and HC concentration versus ignition timing at 3400 RPM and intake manifold pressure of 100 kPa.

Figure 8 shows O<sub>2</sub> and HC concentrations as a function of timing angle. Advanced timing angle caused higher cylinder peak pressure. This higher pressure pushed more fuel- air mixture into the crevices (most significantly, the space between piston crown and cylinder walls) in which the flame was quenched and the mixture was left unburned. Additionally, temperature late in the cycle, when the mixture came out of these crevices, was lower at more advanced ignition timing. The latter temperature meant that hydrocarbons and oxygen did not react, which increased concentration of oxygen in the exhaust and unburned hydrocarbons.

In the Fig. 9, concentrations of carbon monoxide, oxygen and carbon dioxide changed very slightly with ignition timing in the studied range.

**Table 2.** Variation of engine performance for changing condition of ignition time.

Ignition time(before of TDC) [degree]	41	31	21	11
P1(Inlet pressure)[ Kpa]	130	130	130	130
P2(spark pressure)[ Kpa]	998.294	1.47e+003	2.18e+003	3.017e+003
P3(maximum pressure)[ Kpa]	4.29e+003	3.982e+003	3.68e+003	3.52e+003
P4[Kpa]	168.8722	168.469	170.192	173.699
T1(inlet temperature)[ Kelvin]	333	333	333	333
T2(ignition temperature)[ Kelvin]	596.199	666.558	745.658	817.768
Maximum temperature[Kelvin]	1.060e+003	998.835	928.265	863.394
T4[Kelvin]	432.572	431.540	435.954	444.937
Net work[kJ]	0.598	0.602	0.584	0.546
Efficiency[percent]	58.854	59.280	57.4569	53.744



**Fig. 9.** Relationship between O<sub>2</sub>, CO and HC concentrations versus ignition timing. (Intake manifold pressure of 100 kPa and equivalence ratio of unity).

Here, the equivalence ratio was held constant at the ratio of unity; so, there was enough oxygen to react most of the carbon with CO<sub>2</sub>. CO concentration increased and CO<sub>2</sub> concentration decreased when there was not enough oxygen. Some of the carbon monoxide appeared in the exhaust due to frozen equilibrium concentration of CO, O<sub>2</sub> and CO<sub>2</sub>.

Figure 10 shows NO concentration in the exhaust gas versus ignition timing. NO formation depended on temperature. With advancing the ignition timing, the in-cylinder peak pressure increased. The ideal gas law indicated that increase in peak pressure must correspond to the increase in peak temperature and that higher temperature caused the NO concentration to be higher.

The results showed that power tended to increase with spark advance between 17 and 35°CA BTDC. Power was expected to increase with spark advance to a point and then drop off.

The best performance was achieved when the greatest portion of combustion took place near the top dead centre. If the spark was not advanced enough, the piston would already move down when much of the combustion took place. In this case, the ability of expanding this portion of the gas through the full range would be lost which would decrease performance. If ignition was too advanced, too much gas would be burnt while the piston was still increasing. As a result, the work that must be done to compress this gas would decrease the produced net work. These competing effects caused it to be the maximum in power as a function of spark advance.

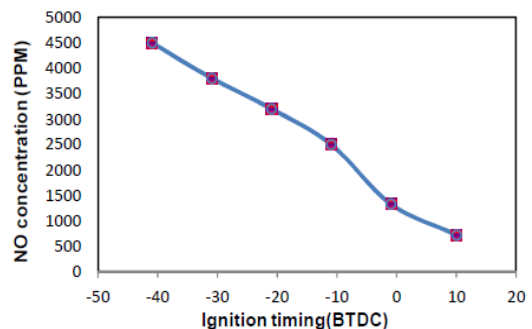


**Fig. 10.** Relationship between NO concentrations versus ignition timing (Engine speed at 3400 RPM and intake manifold pressure of 100 kPa).

Also, it showed that torque increased with increasing ignition advance, which was due to increasing pressure throughout the compression stroke and, consequently, more net work was produced. It is necessary to mention that, by a further increase in spark advance, torque would not increase largely due to in-cylinder peak pressure during compression period and decrease of pressure in expansion stroke. For

this reason, determining the optimum ignition timing is one of the most important characteristics for an SI engine.

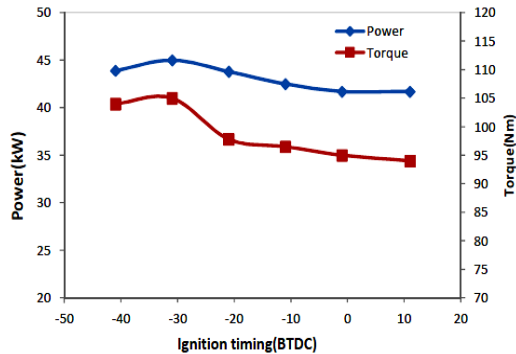


Fig. 11. Relationship between power and torque versus ignition timing.

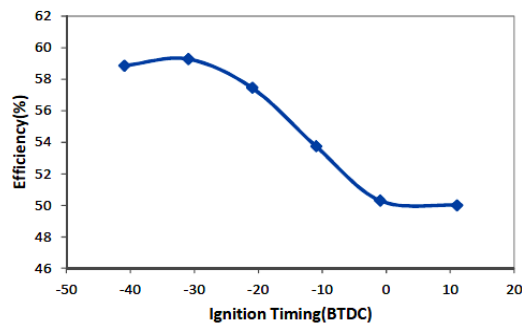


Fig. 12. Relationship between efficiency versus ignition timing.

Figure 12 presents the predicted results of thermal efficiency in comparison with experimental data. Thermal efficiency is work-out divided by energy-in. It can be seen that the net work increased with rising ignition advance to a point and then reduced slightly. This was due to increasing friction at high values of ignition advance and therefore reducing net work. According to Fig. 6, the highest amount to the net work occurred at 31oCA BTDC.

### 7. Conclusions

In this research, during the combustion process, some gasses leak out the cylinder through the rings. This reduction in mass causes a reduction

in enthalpy and engine efficiency. In order to compensate this mass loss, a correction coefficient is needed. Another way is to seal piston and cylinder more precisely. Varying timing angle on the performance of a SI engine shows that by increasing ignition advance, although pressure and temperature increase is happened but because friction losses increase and other losses within an engine, we see heat efficiency and net work decrease. Also in this paper we can see that at 11 degrees before TDC, no knock will be sensed during the engine operation and optimal power and torque is achieved at 31 degrees bTDC. Meanwhile, volumetric efficiency have increased with rising ignition timing but O<sub>2</sub>, CO<sub>2</sub>, CO has been almost constant, but HC with advance of ignition timing increased and the lowest amount NO<sub>x</sub> is obtained at 11 bTDC.

### References

- [1] M. Gölçü, Y. Sekmen and M. Sahir Salman “Artificial neural-network based modeling of variable valve-timing in a spark-ignition engine”, *Applied Energy.*, Vol. 81, pp. 187-197, (2005).
- [2] S. H. Chan and J. Zhu, “Modeling of engine in-cylinder thermodynamics under high values of ignition retard,” *International Journal of Thermal Sciences.*, Vol. 40, No. 1, pp. 94-103, (2001).
- [3] S. Soylu and J. Van Gerpen, “Development of empirically based burning rate sub-models for a natural gas engine,” *Energy Conversion and Management*, Vol. 45, No. 4, pp. 467-481, (2004).
- [4] P. Willard and W., *Engineering Fundamentals of the Internal Combustion Engine*, 2<sup>ed</sup> ed., Prentice Hall, (2003).
- [5] R. Colin Ferguson and T. Kirkpatrick Allan, *Internal Combustion Engines Applied Thermosciences*, John Wiley & Sons, Ins, (2001).
- [6] C. D. Rakopoulos, “Influence of ambient temperature and humidity on

- the performance and emissions of nitric oxide and smoke of high speed Diesel engines in the Athens/Greece region”, *Energy Convers Manage*, Vol. 31, pp. 447-458, (1991).
- [7] D. A. Kouremenos, C. D. Rakopoulos and D. T. Hountalas. “Computer simulation with experimental validation of the exhaust nitric oxide and soot emissions in divided chamber Diesel engines”, *In Proceedings of the ASME-WA meeting* ., 10 (1). San Francisco, CA: AES;. pp. 15-28, (1989).
- [8] H. Hiroyasu, T. Kadota and M. Arai, “Development and Use of a Spray Combustion Modeling to Predict Diesel Engine Efficiency and Pollutant Emissions: Part 2 Computational Procedure and Parametric Study”, *Bulletin of JSME*, Vol. 26, No.214, pp. 576-583, (1983).
- [9] G. H. Abd Alla, H. A Soliman, O. A. Badr and M. F. Abd Rabbo “Effect of injection timing o the performance of a dual fuel engine”, *Journal of Energy conversion and management*, Vol. 43, pp. 269- 277, (2002).
- [10] Y. Zhenzhong, W. Jianqin, F. Zhuoyi and L. Jinding “An investigation of optimum control of ignition timing and injection system in an in-cylinder injection type hydrogen fuelled engine”, *International Journal of Hydrogen Energy*, Vol. 27, pp. 213-217, (2002).